

Supplementary Information

S1. Description of the Integration Method

S1.1. Noise Analysis

The noise level (variance α^2) and autocorrelation (length scale λ) is determined from a sample of the input spectrum where no absorption band is observed and expected. Both parameters are estimated by fitting the autocovariance of the noise with an appropriate covariance function. The autocovariance of the noise \mathbf{x} is calculated for a specific lag (k discrete steps on the wavenumber grid) as follows:

$$\text{COV}(x_n, x_{n+k}) = \frac{1}{N} \sum_{i=1}^{N-k} x_i \cdot x_{i+k} \quad (1)$$

Our spectra are measured on an evenly spaced wavenumber grid, so the lag k can be converted to a wavenumber difference $\tilde{\nu}_j - \tilde{\nu}_i$ by multiplying with the grid spacing (approximately 0.5 cm^{-1}).

To fit the autocovariance and retrieve an approximate relationship for autocovariance versus lag (lag in units of cm^{-1}), we choose the squared exponential covariance function:

$$k(\tilde{\nu}_i, \tilde{\nu}_j) = \alpha^2 \exp\left(-\frac{(\tilde{\nu}_j - \tilde{\nu}_i)^2}{2\lambda^2}\right). \quad (2)$$

The parameter α controls the noise amplitude (variance) and the parameters λ controls how fast the noise correlation of data points i and j decays with distance $\tilde{\nu}_j - \tilde{\nu}_i$ (length scale). These parameters are used to generate random noise samples which have similar characteristics as the experimental noise. A plot of the estimated autocovariance of a sample spectrum and the associated fit is shown in Fig. S1.

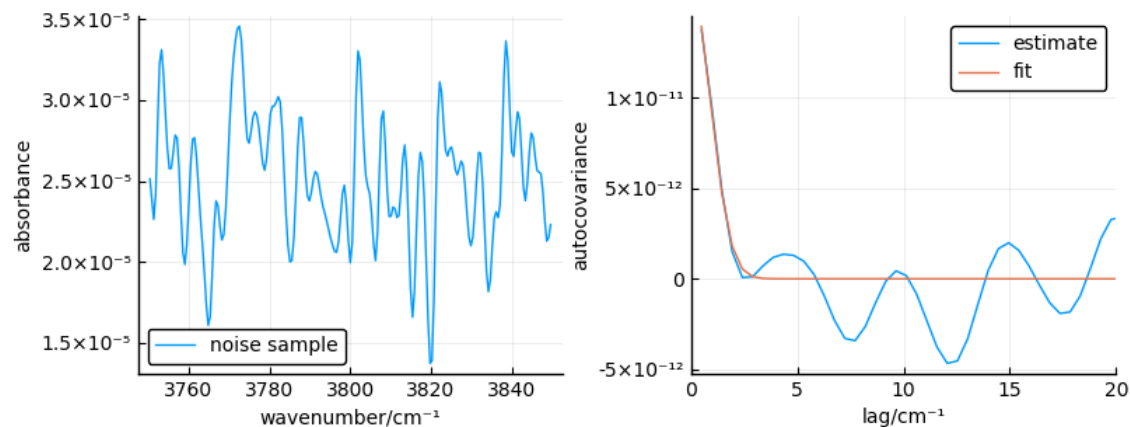


Fig. S1: Noise sample, autocovariance, and fit of squared exponential covariance function.

S1.2. Integration Window Width

The width of the integration window is treated as uncertain and modelled as a random variable W which is sampled from a scaled and shifted (four parameter) Beta distribution¹ with shape parameters $\alpha = 2, \beta = 2$ and scaling and shifting parameters s and m :

$$W \sim \text{Beta}\left(2, 2, m - \frac{s}{2}, m + \frac{s}{2}\right) \quad (3)$$

The symmetric Beta (2, 2) distribution has non-zero probability density in the interval (0,1), peaks at 0.5 (mean value) and goes to zero at the interval bounds. Scaling by s and shifting the mean by m moves this interval such that random samples fall in the range $m - \frac{s}{2} < w < m + \frac{s}{2}$.

The reason to choose a scaled and shifted Beta(2, 2) distribution over a normal distribution is that the tails of the normal distributions would occasionally lead to unreasonable integration boundaries far away from the actual band. A Beta(2, 2) distribution is similar to a normal distribution in that it peaks symmetrically around the mean value but it is missing the tails. A comparison of a scaled and shifted Beta(2, 2) and normal distribution is shown in Fig. S2.

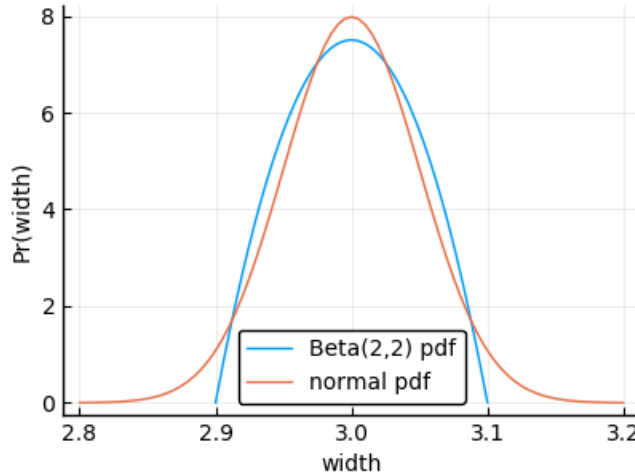


Fig. S2: Example of a probability density function from which random widths for the integration window are drawn (blue trace): A Beta (2,2) distribution scaled by a factor $s = 0.2$ and shifted by $m = 3.0$. Random samples from this distribution fall in the interval (2.9, 3.1), have a mean of 3.0 and a standard deviation of $\frac{\alpha\beta s^2}{(\alpha+\beta)^2(\alpha+\beta+1)} = \sqrt{\frac{1}{20}}s \approx 0.045$.

S1.3. Random Spectra

Spectra with modified noise are generated from a multivariate normal distribution (\mathcal{N}). The multivariate normal distribution is parametrized by a mean vector $\boldsymbol{\mu}$ around which random samples will scatter, and a covariance matrix $\boldsymbol{\Sigma}$ that determines the correlation of the generated sample points. In our case, the absorbance $\mathbf{A}_{\text{input}}$ of the input spectrum serves as mean vector, such that data points in the generated spectra randomly scatter around the data points in the input spectrum. The elements $v_{i,j}$ of the covariance matrix are calculated from the squared exponential covariance function (Eqn. 2).

Random spectra are sampled from the resultant multivariate normal distribution:

$$\mathbf{A} \sim \mathcal{N}(\mathbf{A}_{\text{input}}, \boldsymbol{\Sigma}). \quad (5)$$

After this data generation step we are left with a vector of integration window widths and an associated set of simulated spectra, which are integrated in the next data processing step.

S1.4. Integration

At this point, we introduce several assumptions about the band shape of our FTIR signals:

1. We assume symmetric bands and integrate symmetrically around the band maximum, simply because there is no systematic evidence that suggests asymmetric bands.
2. We assume the same band width for all bands because the complexes we study should have similar rotational constants and rotational temperatures in the jet expansion. Therefore, the mean value m in Eqn. 3 for the width of the integration window is the same for all spectra we analysed, 2.5 cm^{-1} . We assume a 10 % uncertainty for the width of the integration window so that it varies within 0.25 cm^{-1} ($s = 0.1 m$). Note that while the particular value used in each Monte Carlo iteration varies following the Beta distribution introduced above, two bands in the *same* random spectrum are integrated using exactly the same integration window width, which decreases the contribution of the integration window width uncertainty to the overall uncertainty of the band integral ratio.

The numeric integration is performed using the trapezoidal integral approximation. The exact integration boundaries $\tilde{\nu}_a$ and $\tilde{\nu}_b$ ($\tilde{\nu}_a < \tilde{\nu}_b$) generally fall somewhere in between the regular wavenumber grid $\tilde{\nu}_i$ of our FTIR measurements. Therefore, we integrate the interval $[\tilde{\nu}_1 > \tilde{\nu}_a, \tilde{\nu}_2 < \tilde{\nu}_b]$ ($\tilde{\nu}_1$ and $\tilde{\nu}_2$ are points on the wavenumber grid neighboring $\tilde{\nu}_a$ and $\tilde{\nu}_b$) and use linear interpolation to estimate the absorbance at $\tilde{\nu}_a$ and $\tilde{\nu}_b$ to add the remaining two (more narrow) trapezoids. Furthermore, the absorbance at $\tilde{\nu}_a$ and $\tilde{\nu}_b$ is used to determine a slope that is subtracted to account for the local baseline.

To illustrate the integration method, we show the input spectrum, 5 draws of random spectra, integration boundaries and local baselines for the system methanol-phenylacetylene in Fig. S3.

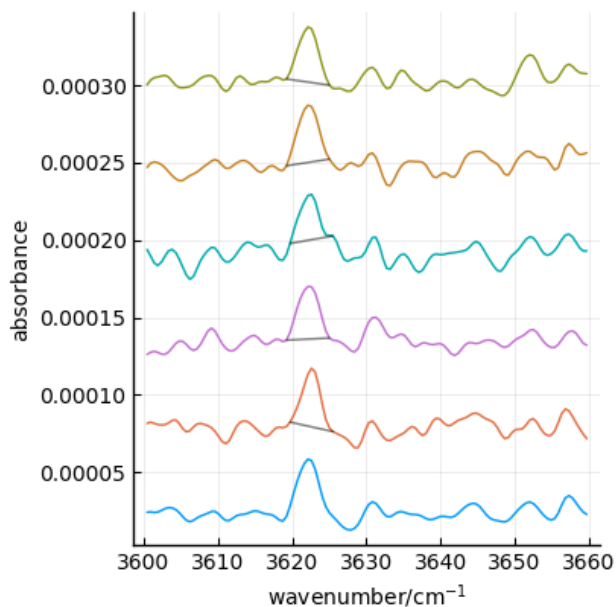
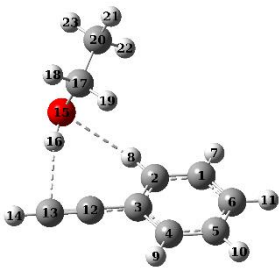
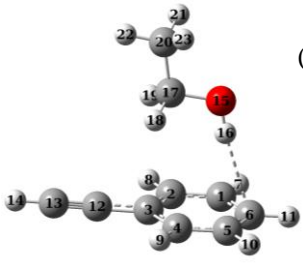
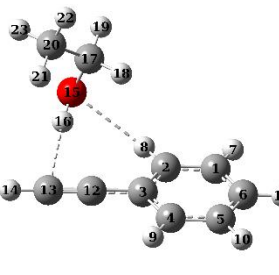
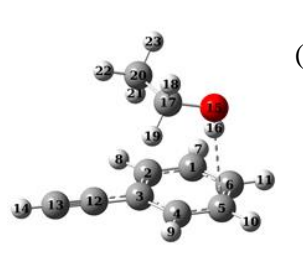
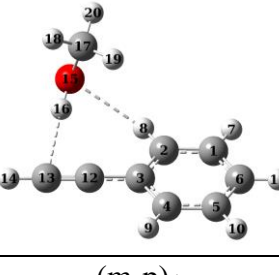
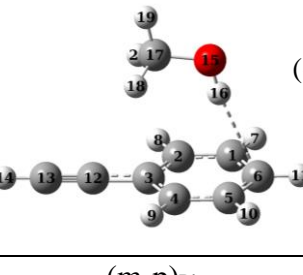
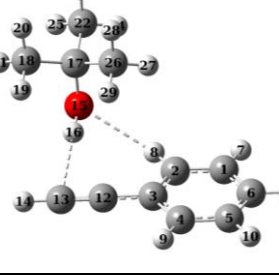
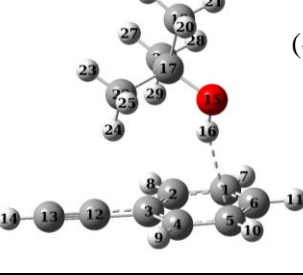
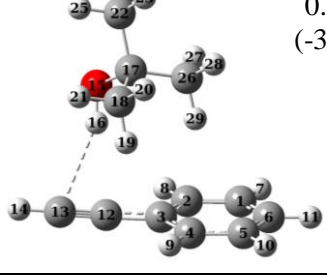
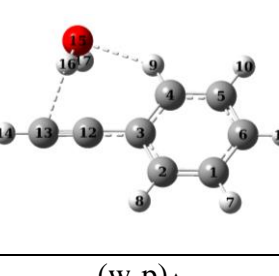
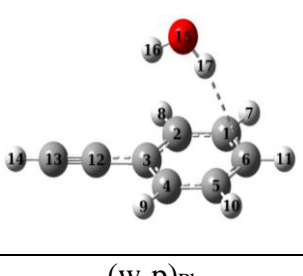


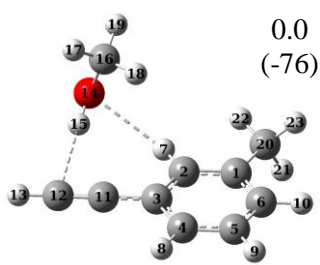
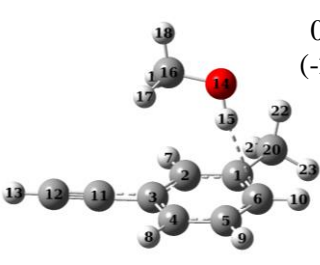
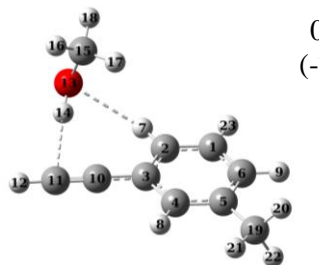
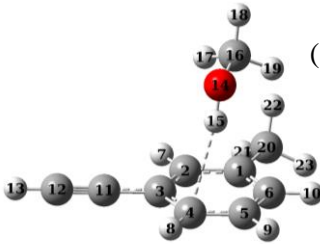

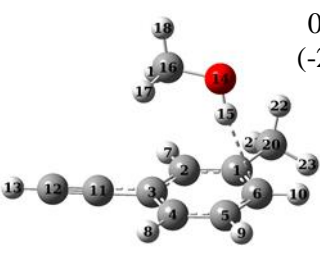
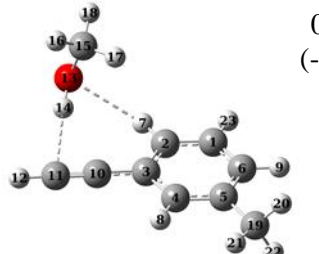
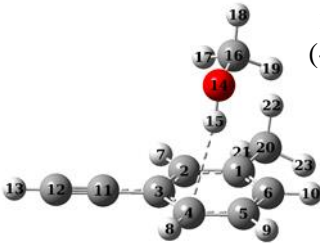
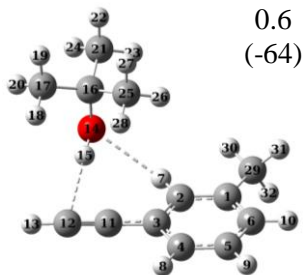
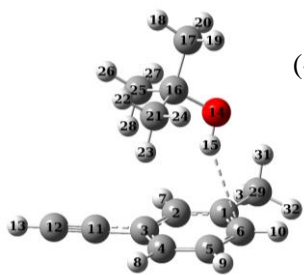
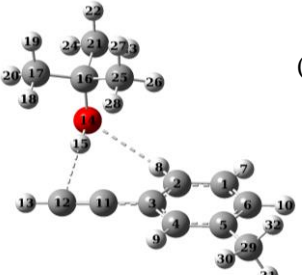
Fig. S3: Input spectrum (lower trace) and 5 random draws for the system methanol-phenylacetylene. The integration boundaries and local baselines are indicated by black lines.

S1.5. Integral Ratio and Confidence Interval

The integration method yields either samples of one band integral or two *associated* integrals (both derived from integration using exactly the same width). The latter is the trivial case: We calculate the ratios of the associated integrals and can calculate the mean and standard deviation as well as 95% confidence intervals from 2.5 % and 97.5 % quantiles from the sample of retrieved ratios. However, with the present dataset we have many spectra where only the band of the acetylene- or the phenyl-bound complex is observable. While this already establishes the energetic preferences of binding sites, we still wish to estimate a bound for the intensity ratio and finally the abundance ratio of the two species. To do so, we use the confidence interval of the integral of the observed band: For a signal to be viewed as a true absorption band and not a noise artefact, we demand that the 5.0 % quantile of the distribution over integral samples is > 0 , i.e. that there is a 95% probability that the band integral is > 0 . Given that the absorption bands of the two phenyl- and acetylene-bound complexes are spectral "neighbours" and are perturbed by noise with identical characteristics, we can assume that the width of the distribution over integral samples should be similar for both bands. This was verified using our measurements where both bands are observable. Therefore, shifting the histogram of the observed bands' integrals such that the 5 % quantile lands on zero yields an upper bound for how the distribution of the unobserved band may look like. The 97.5 % quantile of this hypothetical distribution is equal to the quantile difference $q_{97.5} - q_{5.0}$ of the observed bands' distribution and it is an estimate of the upper bound of the integral of the unobserved band.

S2. Calculated and Experimental Results

Ac Minima	Ph Minima	Local Minima
 <p>0.0 (-67)</p>	 <p>1.5 (-16)</p>	
(e _t -p) _{Ac}	(e _t -p) _{Ph}	
 <p>0.0 (-64)</p>	 <p>0.9 (-17)</p>	
(e _g -p) _{Ac}	(e _g -p) _{Ph}	
 <p>0.0 (-73)</p>	 <p>1.4 (-16)</p>	
(m-p) _{Ac}	(m-p) _{Ph}	
 <p>0.0 (-62)</p>	 <p>1.3 (-16)</p>	 <p>0.8 (-37)</p>
(t-p) _{Ac}	(t-p) _{Ph}	(t-p) _{Ac2}
 <p>0.0 (-54)</p>	 <p>0.6 (-5)</p>	
(w-p) _{Ac}	(w-p) _{Ph}	

Ac Minima	Ph Minima	Local Minima
 <p>0.0 (-76)</p>	 <p>0.5 (-27)</p>	 <p>0.7 (-75)</p>
(m-3mp) _{Ac}	(m-3mp) _{Ph}	(m-3mp) _{Ac2}
		 <p>2.4 (-30)</p>
		(m-3mp) _{Ph2}
 <p>0.0 (-57)</p>	 <p>0.7 (-21)</p>	 <p>0.7 (-56)</p>
(md-3mp) _{Ac}	(md-3mp) _{Ph}	(md-3mp) _{Ac2}
		 <p>2.7 (-23)</p>
		(md-3mp) _{Ph2}
 <p>0.6 (-64)</p>	 <p>0.0 (-16)</p>	 <p>1.7 (-63)</p>
(t-3mp) _{Ac}	(t-3mp) _{Ph}	(t-3mp) _{Ac2}

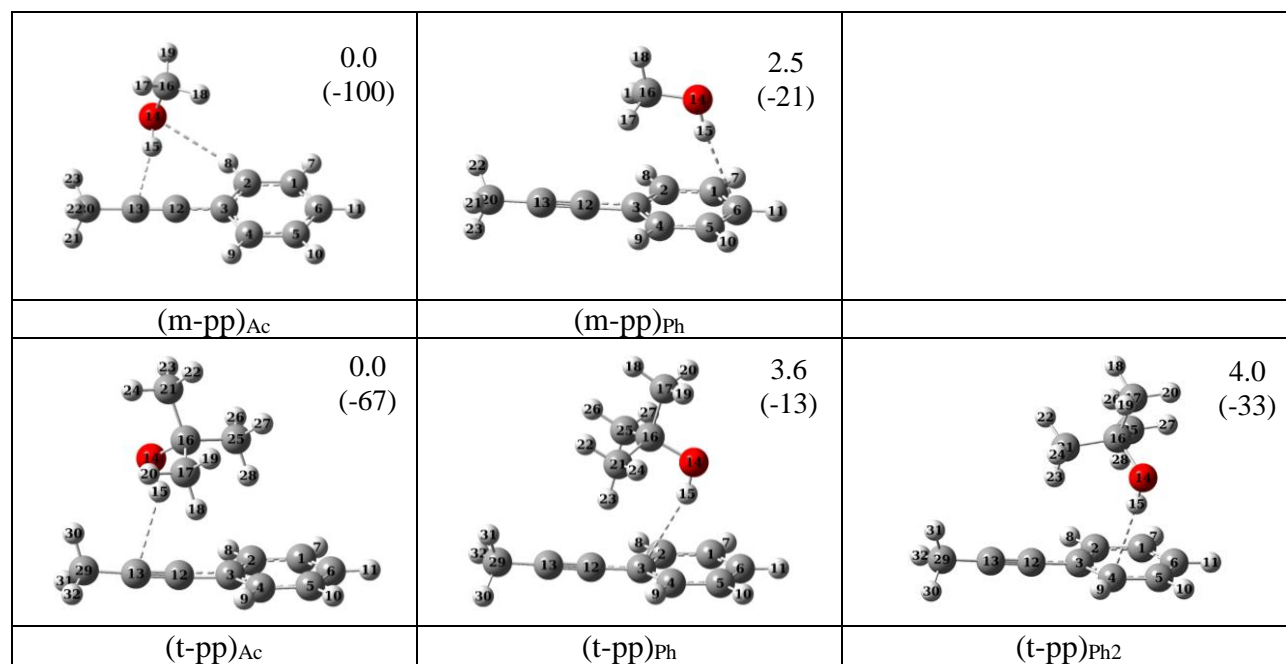


Fig. S4: Optimized structures of phenyl bound (Ph) and acetylenic bound (Ac) complexes of various donor molecules (e_t and e_g represent ethanol in trans and gauche-conformation respectively, m: methanol, md: methanol- d_1 , t: *tert*-butyl alcohol, w: H_2O) with phenylacetylene (p), 3-methylphenylacetylene (3mp) and 1-phenyl-1-propyne (pp) are given at B3LYP-D3/def2-TZVP level. The upper number in each block represent the relative ZPVE corrected energies in kJ mol^{-1} . The number in parenthesis indicates the scaled computed wavenumber downshift (cm^{-1}) in the OH stretching fundamental of the donor molecule on complex formation.

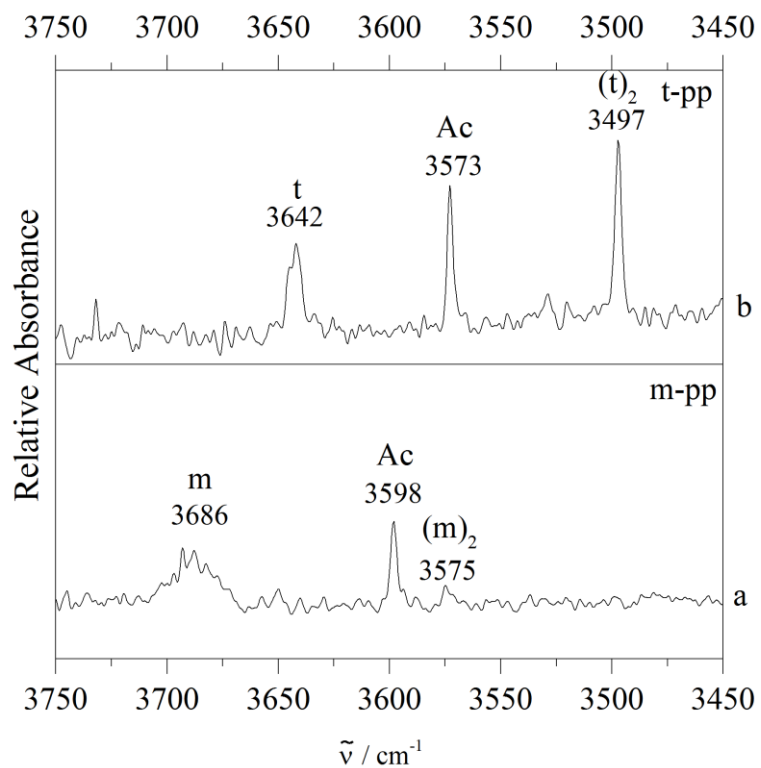


Fig. S5: FTIR spectra of supersonic jet expansions of methanol (m) or *tert*-butyl alcohol (t) with 1-phenyl-1-propyne (pp) in the OH stretching region of the alcohol. (a) Co-expansion of m with pp. (b) Co-expansion of t with pp. Ac indicates the acetylenic bound binary complex. Bands of monomers and homodimer complexes are marked as m, (m)₂ and t, (t)₂, respectively.

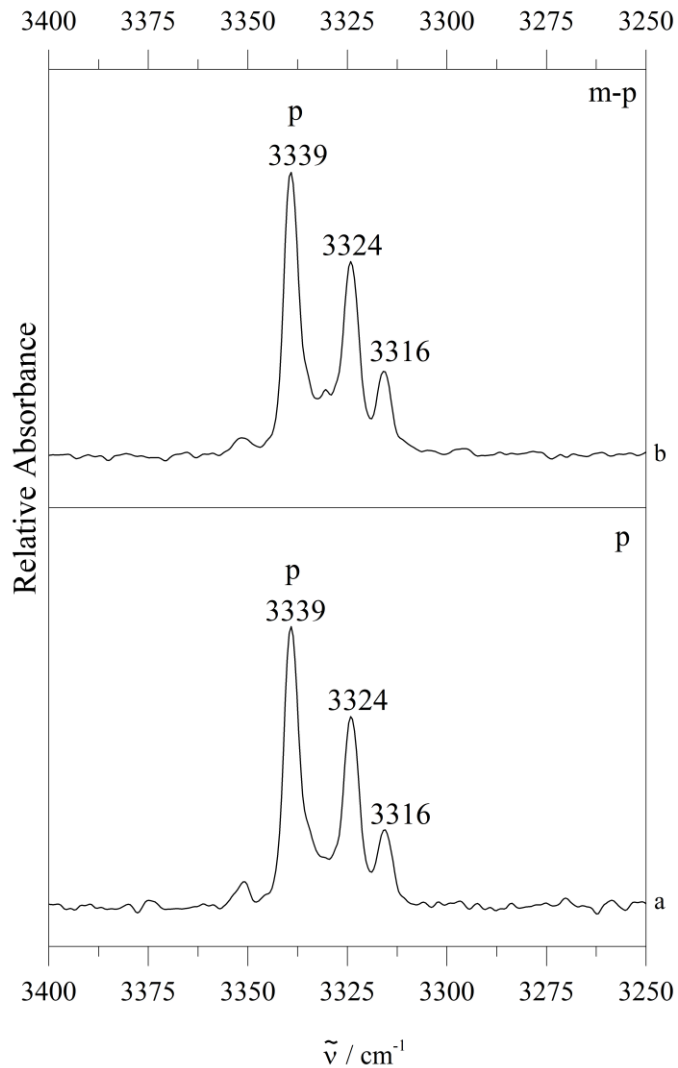


Fig. S6: FTIR spectra of supersonic jet expansions of methanol (m) with phenylacetylene (p) in the $\equiv\text{CH}$ stretching region of p. (a) Spectrum of p. (b) Co-expansion of m with p. The $\equiv\text{CH}$ stretch of monomer is marked as p and occurs at 3339 cm^{-1} together with a Fermi resonance component at 3324 cm^{-1} which is reported to be due to coupling between $\equiv\text{C-H}$ stretch and the combination band arising out of one quantum of $\text{C}\equiv\text{C}$ stretch and two quanta of $\text{C}\equiv\text{C-H}$ out-of-plane bend. The shoulder at 3316 cm^{-1} is due to higher order coupling.²

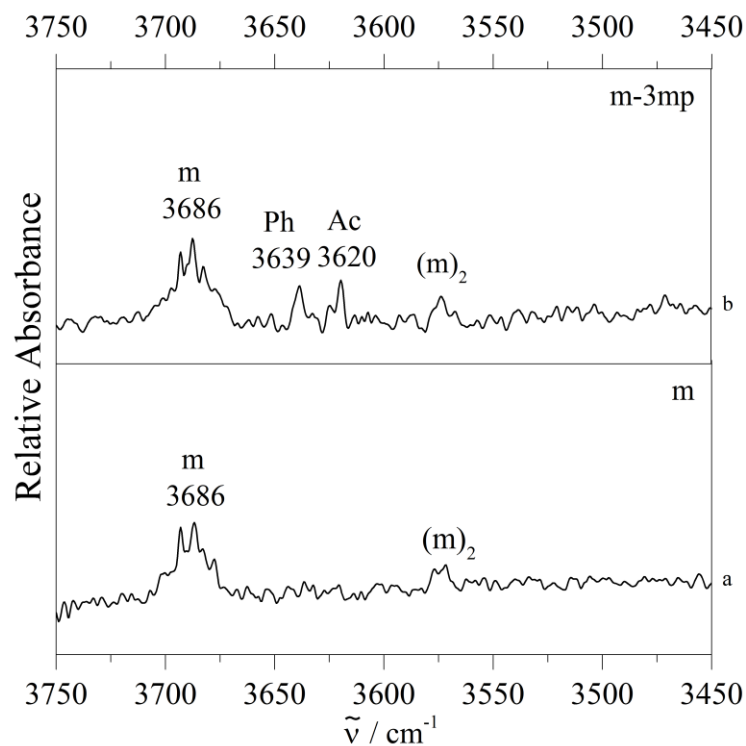


Fig. S7: FTIR spectra of supersonic jet expansions of methanol (m) with 3-methylphenylacetylene (3mp) in the OH stretching region of m. (a) Spectrum of m. (b) Co-expansion of m with 3mp. Ac indicates the acetylenic bound and Ph indicates the phenyl bound binary complex. Bands of monomers and homodimer complexes are marked as m and $(m)_2$, respectively.

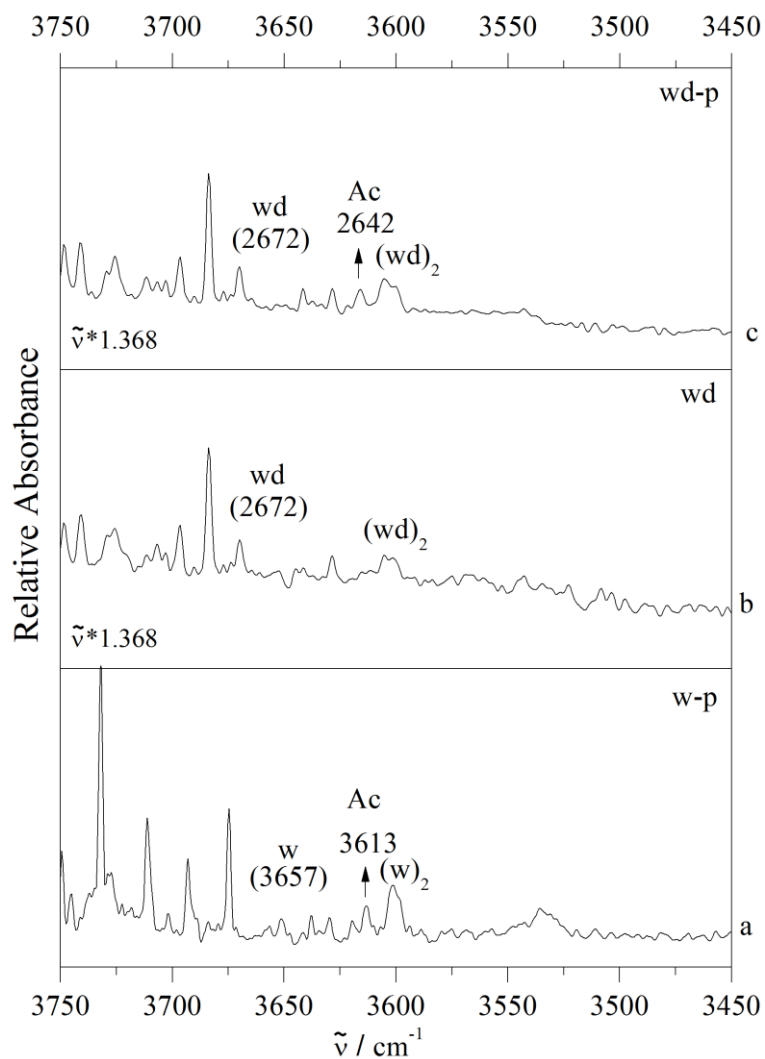


Fig. S8: FTIR spectra of supersonic jet expansions of water (w) with phenylacetylene (p) in the OH stretching region of w. (a) Co-expansion of w with p. (b) Spectrum of D₂O (wd). The OD stretch region of wd is scaled to the OH stretch region of w by using a scaling factor of 1.368 (3657/2672). (c) Co-expansion of wd with p. Ac indicates the acetylenic bound binary complex. Bands of monomers and homodimer complexes are marked as w, wd and (w)₂, (wd)₂, respectively.

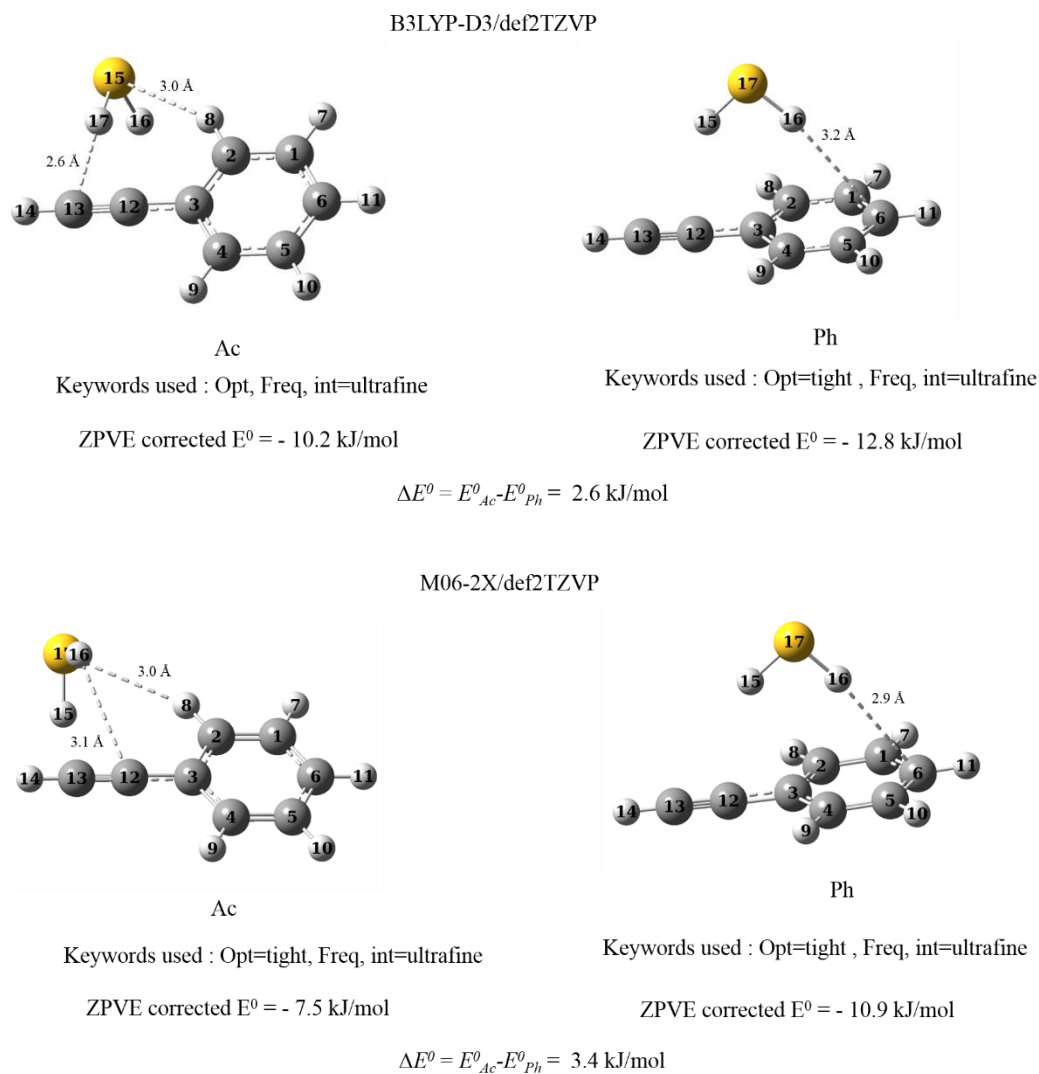


Fig. S9: Optimized structures of phenyl bound (Ph) and acetylenic bound (Ac) complexes of H₂S with phenylacetylene (p) are given at B3LYP-D3/def2-TZVP and M06-2X/ def2-TZVP level.

Table S1. Calculated harmonic, experimentally scaled wavenumbers ω_{OH}^f in cm^{-1} of donor monomers, scaled wavenumber shifts $\Delta\omega_{OH}^f$ in cm^{-1} , integrated band strengths (σ_{OH}) in the double harmonic approximation in km mol^{-1} and ZPVE corrected binding energies E^0 in kJ mol^{-1} of phenyl bound (Ph) and acetylenic bound (Ac) complexes are given at B3LYP-D3/def2-TZVP level. Experimental anharmonic wavenumber shifts based on the assignments proposed here are added in parentheses behind the calculated harmonic shifts, showing a systematic underestimation of the calculated shift magnitude for Ph binding and a slight systematic overestimation for Ac binding. For the two e isomers, similar complexation shifts are predicted, but because e_g is experimentally 16 cm^{-1} lower, an e_t assignment of the observed band is more consistent with other alcohols.

Donor	Monomer			Complex	Coordination					
	$\omega_{OH}^f/\text{cm}^{-1}$	$\sigma_{OH}/\text{km mol}^{-1}$	f Scaling Factor		Ph			Ac		
					$E^0/\text{kJ mol}^{-1}$	$\Delta\omega_{OH}^f/\text{cm}^{-1}$	$\sigma_{OH}/\text{km mol}^{-1}$	$E^0/\text{kJ mol}^{-1}$	$\Delta\omega_{OH}^f/\text{cm}^{-1}$	$\sigma_{OH}/\text{km mol}^{-1}$
e_t	3676	23	0.9646	e_t -p	-18.76	-16	122	-20.25	-67 (-62)	178
e_g	3660	18	0.9644	e_g -p	-19.50	-17	98	-20.42	-64 (-46)	163
m	3686	25	0.9667	m-p	-18.23	-16	115	-19.60	-73 (-64)	191
t	3642	12	0.9615	t-p	-20.03	-16	124	-21.35	-62 (-55)	192
wd*	2672	4	0.9795	wd-p**	-15.19	-2	20	-16.33	-34 (-30)	57
md*	2718	18	0.9791	md-3mp	-20.18	-21 (-33)	79	-20.92	-57 (-47)	110
w	3657	4	0.9695	w-p**	-14.49	-5	32	-15.11	-54 (-44)	122
m	3686	25	0.9667	m-3mp	-19.96	-27 (-47)	132	-20.45	-76 (-66)	186
td*	2687	9	0.9746	td-3mp	-23.30	-12 (-28)	73	-22.96	-47	106
t	3642	12	0.9615	t-3mp	-23.17	-16 (-41)	124	-22.58	-64	186
m	3686	25	0.9667	m-pp	-19.43	-21	21	-21.91	-100 (-88)	103
t	3642	12	0.9615	t-pp	-21.86	-13	14	-25.41	-67 (-69)	70

* The OD stretch of the donor is considered in these deuterated variants.

** In case of w and wd the shift is calculated from the symmetric OH and OD monomer stretch, respectively.

Table S2. Calculated harmonic experimentally scaled wavenumbers ω_{OH}^f in cm^{-1} of donor monomers, scaled wavenumber shifts $\Delta\omega_{OH}^f$ in cm^{-1} , relative band strengths (σ_{OH}) in the double harmonic approximation in km mol^{-1} and ZPVE corrected binding energies E^0 in kJ mol^{-1} of phenyl bound (Ph) and acetylenic bound (Ac) complexes are given at M06-2X/def2-TZVP level. Experimental anharmonic wavenumber shifts based on the assignments proposed here are added in parentheses behind the calculated harmonic shifts, showing a systematic underestimation of the calculated shift magnitude for Ph binding and Ac binding. Therefore, in some cases Ac binding may be predicted to be closer to experimental Ph binding in terms of shift and experimental Ac binding would remain unexplained in terms of shift. For the two e isomers, similar complexation shifts are predicted. Taking into account that isolated e_g is experimentally 16 cm^{-1} lower, both assignments are reasonably consistent with other alcohols. Therefore, a spectral assignment based on M06-2X remains ambiguous.

Donor				Complex	Coordination					
					Ph			Ac		
	$\omega_{OH}^f/\text{cm}^{-1}$	$\sigma_{OH}/\text{km mol}^{-1}$	f Scaling Factor		$E^0/\text{kJ mol}^{-1}$	$\Delta\omega_{OH}^f/\text{cm}^{-1}$	$\sigma_{OH}/\text{km mol}^{-1}$	$E^0/\text{kJ mol}^{-1}$	$\Delta\omega_{OH}^f/\text{cm}^{-1}$	$\sigma_{OH}/\text{km mol}^{-1}$
e_t	3676	37	0.9445	e_t -p	-18.39	-27	127	-18.34	-46 (-62)	126
e_g	3660	30	0.9450	e_g -p	-19.65	-27	97	-18.99	-41 (-46)	111
m	3686	41	0.9466	m-p	-17.64	-28	118	-17.77	-45 (-64)	134
t	3642	22	0.9438	t-p	-19.19	-18	121	-19.24	-51 (-55)	173
wd*	2672	8	0.9594	wd-p**	-15.49	-12	27	-14.88	-27 (-30)	54
md*	2718	28	0.9587	md-3mp	-19.93	-23 (-33)	75	-19.02	-37 (-47)	81
w	3657	12	0.9464	w-p**	-14.62	-17	43	-13.80	-42 (-44)	115
m	3686	41	0.9466	m-3mp	-19.78	-29 (-47)	124	-18.57	-48 (-66)	134
td*	2687	14	0.9566	td-3mp	-21.55	-14 (-28)	72	-20.64	-37	99
t	3642	22	0.9438	t-3mp	-21.47	-18 (-41)	121	-20.25	-51	173

*The OD stretch of the donor is considered in these deuterated variants.

** In case of w and wd the shift is calculated from the symmetric OH and OD monomer stretch, respectively.

References

1. N. L. Johnson, S. Kotz and N. Balakrishnan, *Continuous Univariate Distributions Vol. 2 (2nd ed.)*, Wiley, New York, 1995.
2. J. A. Stearns and T. S. Zwier, Infrared and Ultraviolet Spectroscopy of Jet-Cooled ortho-, meta-, and para-Diethynylbenzene, *J. Phys. Chem. A*, 2003, **107**, 10717-10724.